JOURNAL OF SOLID STATE CHEMISTRY 91, 113–120 (1991)

Synthesis, Structural Characterization, and Two-Dimensional Antiferromagnetic Ordering for the Oxides $Ti_{3(1-x)}Ni_xSb_{2x}O_6$ ($1.0 \geq x \geq 0.6$)

E. RAMOS, M. L. VEIGA, F. FERNÁNDEZ, R. SÁEZ-PUCHE, AND C. PICO

Departamento de Química Inorgánica I, Facultad de Ciencias Químicas, Universidad Complutense, 28040-Madrid, Spain

Received July 25, 1990; in revised form October 29, 1990

A new family of mixed oxides of general formula $Ti_{3(1-x)}Ni_xSb_{2x}O_6$ for $1.0 \geq x \geq 0.6$ has been synthesized, by solid state reaction in air, and the crystallographic data for these oxides have been determined. The structures of these compounds are related to the rutile or trirutile type structure. Magnetic susceptibility measurements, between 4.2 and 300 K, show the existence of a broad maximum centered at about 35 K for the $NiSb_2O_6$ oxide which has been fitted by using the high temperature series expansion method (HTSE) and the estimated value of the exchange integral is -7 K. This bidimensional antiferromagnetic ordering is drastically lowered when the x value increases for the different doped phases in the system $Ti_{3(1-x)}Ni_xSb_{2x}O_6$.

Introduction

The compounds of the general formula AB_2O_6, where A is Mg or a certain $3d$ divalent cation (*1*) and B = Nb, Ta, and Sb with an oxidation state of five, adopt the trirutile type structure, sometimes described as the Tapiolite structure, after the mineral of that name, $FeTa_2O_6$. The chains of octahedra $[BO_6]$ have the atoms of the divalent cation, in a regular sequence in the vertical direction: A^{2+}–B^{5+}–B^{5+}–A^{2+}, which leads to a tripled c parameter (Fig. 1a). The structure found is tetragonal with space group $P4_2/mnm$ (No. 136) (*2*, *3*).

This structure can be related to the layered K_2NiF_4 type. In both cases the main feature is the bidimensional arrangement of the magnetic cations B. The existence of short-range magnetic correlations has been reported for MTa_2O_6 (M = Fe, Co, and Ni) (*4*).

Neutron diffraction and magnetic susceptibility studies for both $CoTa_2O_6$ and $CoSb_2O_6$ have revealed the existence of antiferromagnetic ordering which has been explained by means of the two-dimensional Ising model (*5*). The differences in the magnetic behavior between both oxides have been explained by considering the different bond distances within the Co–O layers.

In the case of the homologous $NiSb_2O_6$, neither a detailed crystal study nor magnetic measurements have been reported. In the present study the substitution of Ni by a diamagnetic Ti^{4+} ion to give the sample composition $Ti_{3(1-x)}Ni_xSb_{2x}O_6$ is achieved.

0022-4596/91 $3.00

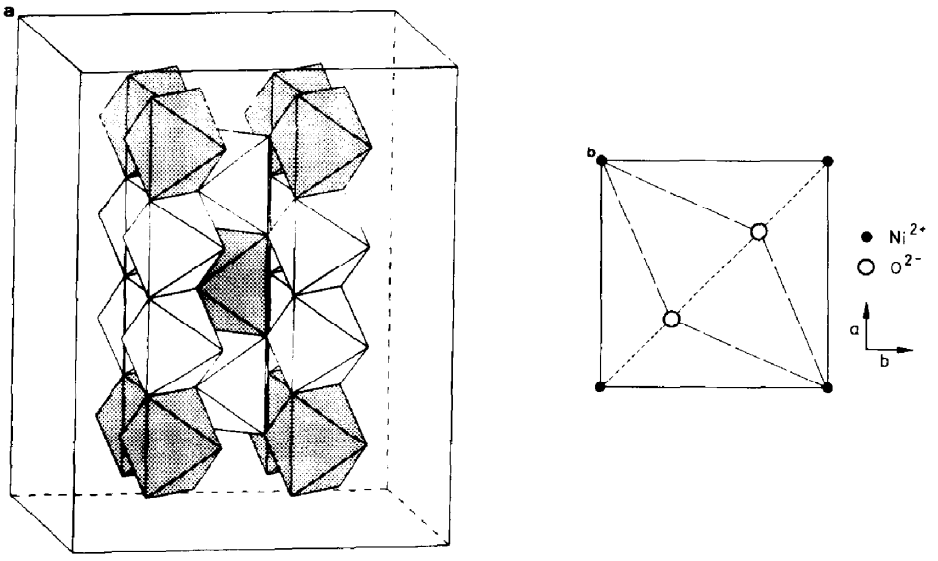

FIG. 1. (a) Structural model for $NiSb_2O_6$. Coordination polyhedra of Ni (shaded) and Sb (white). (b) Superexchange pathways for $NiSb_2O_6$ trirutile. The dashed and dotted lines represent the Ni–O–Ni and Ni–O–O–Ni interactions, respectively.

Experimental

Polycrystalline materials (yellow greenish color) $Ti_{3(1-x)}Ni_xSb_{2x}O_6$ ($1.0 \geq x \geq 0.6$) were obtained from a mixture of powders of $NiCO_3$ (Merck), Sb_2O_5 (*6*), and TiO_2 (Merck), in stoichiometric amounts by heating in air initially at 1000 K for 24 hr and finally at 1050 K for 5 days (*7*).

Powder X-ray diffraction patterns were registered at a rate of 0.1 (2θ) min^{-1} by means of a Siemens Kristalloflex powder diffractometer by a D500 generator using Ni-filtered Cu$K\alpha$ radiation. A 2θ step size of 0.04° was used, and the Rietveld's profile analysis method (*8*) was utilized for refinement of X-ray diffraction results in these materials.

IR absorption spectra were recorded with a Perkin–Elmer 1320 spectrophotometer in the wavenumber range 4000–200 cm^{-1} using KBr pellets.

The magnetic susceptibility measurements (χ) were made using a susceptometer DSM5 described elsewhere (*9*). The setup based on the Faraday method was calibrated with $Hg[Co(SCN)_4]$ and $Gd_2(SO_4)_3 \cdot 8H_2O$ as standards and χ was independent of the temperature range of measurements. The maximum magnetic field was 14 kG with $H\,dH/dz = 30\ kG^2\ cm^{-1}$.

The susceptibilities were corrected for ionic diamagnetism using the values in 10^{-6} emu $\cdot$ mol^{-1}, 16 for O^{2-}, 5 for Ti^{4+}, 12 for Ni^{2+}, and 14 for Sb^{5+} (*10*).

Results and Discussion

From the experimental conditions given above, a trirutile solid solution $Ti_{3(1-x)}Ni_xSb_{2x}O_6$, with a wide composition range $1.0 < x < 0.6$ has been isolated. The expected trirutile structure was verified in all cases. The lattice parameters have been refined by us with respect to those proposed by Kasper (*11*) for $NiSb_2O_6$ from X-ray diffraction work.

The a and c parameters decrease progres-

TABLE I

CRYSTALLOGRAPHIC DATA OF THE OXIDES $Ti_{3(1-x)}Ni_xSb_{2x}O_6$ ($0.6 \leq x \leq 1.0$)

$Ti_{3(1-x)}Ni_xSb_{2x}O_6$	a (Å)	c (Å)	c/a	d_{cal} ($g \cdot cm^{-3}$)	d_{exp} ($g \cdot cm^{-3}$)
$x = 1$	4.641(2)	9.219(6)	1.9857	6.66	6.67
$x = 0.9$	4.638(5)	9.198(6)	1.9828	6.41	6.45
$x = 0.8$	4.637(6)	9.197(2)	1.9829	6.15	6.19
$x = 0.7$	4.637(4)	9.196(1)	1.9830	5.88	6.01
$x = 0.6$	4.635(8)	9.191(1)	1.9826	5.62	5.63

sively with x (Table I). Taking into account the ionic radius values, this fact is concordant with the substitution of Ni(II) (0.69 Å) and Sb(V) (0.60 Å) by Ti(IV) (0.605 Å) (*12*). The crystallographic data of $NiSb_2O_6$ and $Ti_{1.2}Ni_{0.6}Sb_{1.2}O_6$, first and last members of this series, are shown in Tables II and III. The agreement between the observed and the calculated diffraction profiles for $NiSb_2O_6$ and $Ti_{1.2}Ni_{0.6}Sb_{1.2}O_6$ are depicted on Figs. 2a and 2b. The structural model is given in Fig. 1a. The bond lengths (or distances) and angles for these compounds are shown in Tables IV and V. The examination of these results suggests a progressive distortion of the BO_6 octahedra exhibiting two short bonds and four long similar bonds in the SbO_6 octahedra. The tetragonal distortion observed in SbO_6 can be justified by taking into account the size of Sb(V) with respect to those of Nb(V) and Ta(V).

TABLE II

CRYSTALLOGRAPHIC PARAMETERS OF $NiSb_2O_6$

Atom	Position	x	y	z	N
Ni	$2a$	0	0	0	0.125
Sb	$4e$	0	0	0.3317(2)	0.25
O(1)	$4f$	0.3032(4)	0.3032(4)	0	0.25
O(2)	$8j$	0.3014(6)	0.3014(6)	0.3290(6)	0.50

R_p [a]	11.10%
R_{wp} [b]	15.02%
R_b [c]	5.91%
R_{exp} [d]	5.15%
χ^2 [e]	8.51%
No. of data points	2701
Limits of angle	12–119°
No. of reflections	94

Note. Space group $P4_2/mnm$; $Z = 2$; $a = 4.641(2)$ Å; $b = 9.219(6)$ Å; Vol = 198.6(1) Å^3.
[a] $R_p = 100\Sigma_i (Y_i - Y_{ci})/\Sigma_i (Y_i)$.
[b] $R_{wp} = [100\Sigma_i (Y_i - Y_{ci})^2/\Sigma_i (Y_i)^2]^{1/2}$.
[c] $R_b = 100\Sigma_i (I_i - I_{ci})/\Sigma_i (I_i)$.
[d] $R_{exp} = 100[N - P + C/\Sigma_i W_i Y_i^2]^{1/2}$.
[e] $\chi^2 = (R_{wp} - R_{exp})^2$.

TABLE III

CRYSTALLOGRAPHIC PARAMETERS OF THE $Ti_{1.2}Ni_{0.6}Sb_{1.2}O_6$

Atom	Position	x	y	z	N
Ni/Ti	$2a$	0	0	0	0.075/0.05
Sb/Ti	$4e$	0	0	0.330(6)	0.15/0.10
O(1)	$4f$	0.296(5)	0.296(5)	0	0.25
O(2)	$8j$	0.312(4)	0.312(4)	0.345(3)	0.50

R_p [a]	19.5%
R_{wp} [b]	22.4%
R_b [c]	6.79%
R_{exp} [d]	14.5%
χ^2 [e]	2.39%
No. of data points	2751
Limits of angle	10–119°
No. of reflections	98

Note. Space group $P4_2/mnm$; $Z = 2$; $a = 4.635(8)$ Å; $c = 9.191(1)$; Vol = 197.5(2) Å^3.
[a] $R_p = 100\Sigma_i (Y_i - Y_{ci})/\Sigma_i (Y_i)$.
[b] $R_{wp} = [100\Sigma_i (Y_i - Y_{ci})^2/\Sigma_i (Y_i)^2]^{1/2}$.
[c] $R_b = 100\Sigma_i (I_i - I_{ci})/\Sigma_i (I_i)$.
[d] $R_{exp} = 100[N - P + C/\Sigma_i W_i Y_i^2]^{1/2}$.
[e] $\chi^2 = (R_{wp} - R_{exp})^2$.

The IR absorption spectra seem to support the above structural results (Fig. 3); thus we can define two zones in the spectra, according to (*13*, *15*): stretching (Sb–O) bands in the region 700–500 cm^{-1} and bending (O–Sb–O) bands in the region 350–200 cm^{-1}. The symmetric stretching vibrations are shown by the bands centered at 700 cm^{-1} and those registered in the 500–600 cm^{-1} range. The more intense splitting observed for $x = 0.8$ in the latter region can be attributed to the progressive substitution of Sb(V) by the other metals in octahedral sites (*16*). The antisymmetric modes Sb–O appear at 630 cm^{-1}. The bending motions are registered in a strong broad absorption toward 340 cm^{-1} (symmetric) and a medium band at 290 cm^{-1} (antisymmetric). Also this

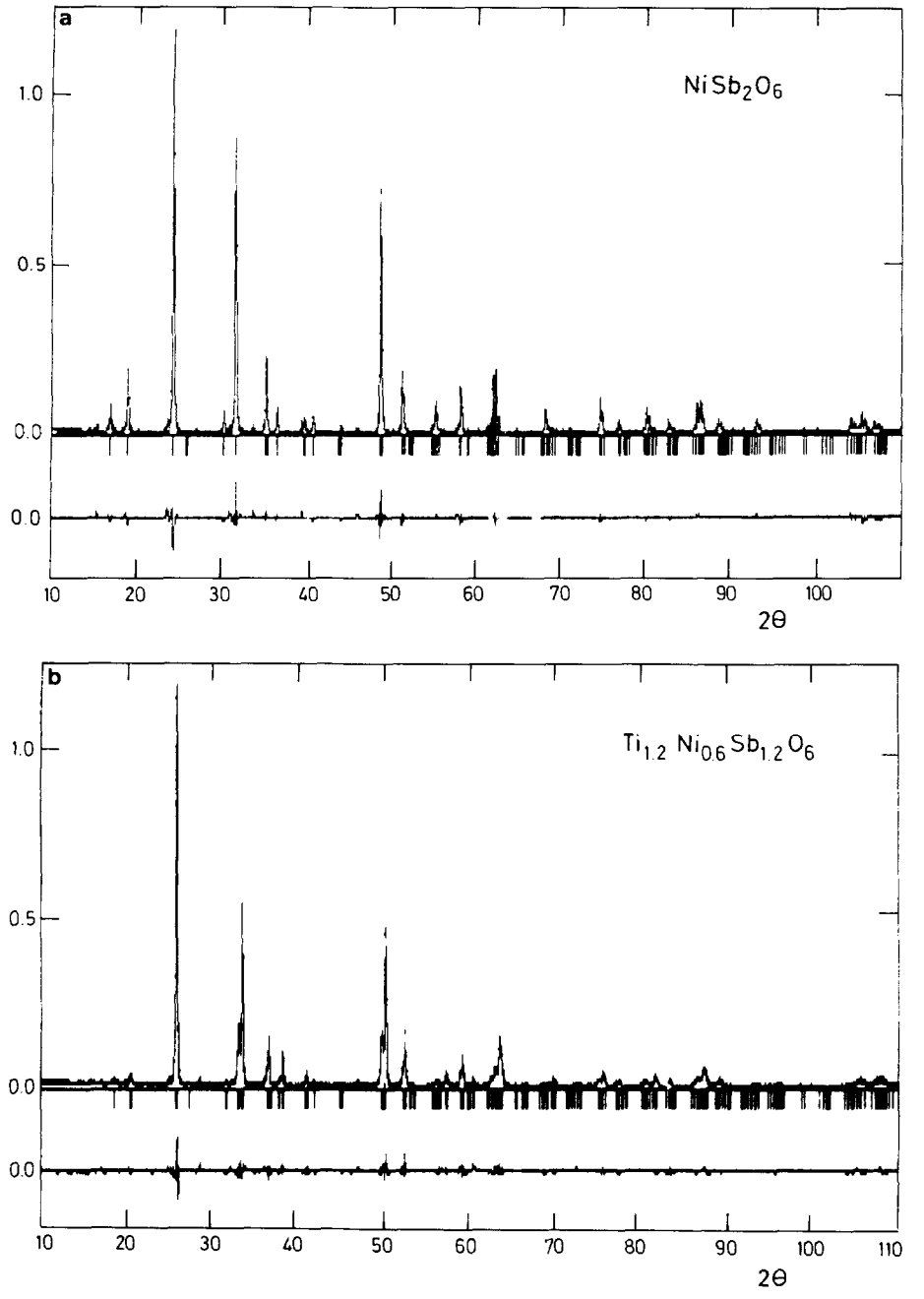

FIG. 2. (a) The observed (· · ·), calculated (—) and difference diffraction profiles for $NiSb_2O_6$. (b) The observed (· · ·), calculated (—) and difference diffraction profiles for $Ti_{1.2}Ni_{0.6}Sb_{1.2}O_6$.

TABLE IV

BOND DISTANCES AND ANGLES FOR $NiSb_2O_6$

Bond	Distance (Å)	Expected (Å)	Angle (°)
Ni–O	Ni–O_1 1.990(1)	2.05(3)	O_1–Ni–O_1 180.00(0)
	Ni–O_2 2.045(7)		O_1–Ni–O_2 90.00(0)
			O_2–Ni–O_2 180.00(0)
			O_2–Ni–O_2 100.71(5)
			O_2–Ni–O_2 79.28(4)
Sb–O	Sb–O_1 1.973(4)	1.98(2)	O_1–Sb–O_1 79.61(1)
	Sb–O_2 1.978(6)		O_1–Sb–O_2 178.41(6)
	Sb–O_2 2.019(1)		O_1–Sb–O_2 98.79(4)
			O_1–Sb–O_2 90.55(4)
			O_2–Sb–O_2 178.55(6)
			O_2–Sb–O_2 89.45(8)
			O_2–Sb–O_2 82.79(9)

latter band is split in two well-defined absorptions for the $x = 0.8$ member.

It is possible to distinguish a light displacement when the Ti(IV) content due to the smaller electronegativity of this ion increases in comparison with Sb.

In addition to the above structural results, some comments relative to the characterization of the more substituted materials ($x = 0.8$) are necessary. First, the X-ray diffraction results cannot be attributable unambiguously to single phases and the Rietveld's analysis suggests the presence of rutile and

TABLE V

BOND DISTANCES AND ANGLES FOR $Ti_{1.2}Ni_{0.6}Sb_{1.2}O_6$

Bond	Distance (Å)	Angle (°)
Ni–O	Ni–O_1 1.942(6)	O_1–Ni–O_1 180.00(0)
	Ni–O_2 1.873(6)	O_1–Ni–O_2 90.00(0)
		O_2–Ni–O_2 81.69(0)
		O_2–Ni–O_2 98.31(0)
		O_2–Ni–O_2 180.00(0)
Sb–O	Sb–O_1 2.049(2)	O_1–Sb–O_1 81.34(1)
	Sb–O_1 2.057(3)	O_1–Sb–O_2 87.10(4)
	Sb–O_2 2.034(5)	O_1–Sb–O_2 102.29(7)
		O_1–Sb–O_2 176.36(3)
		O_2–Sb–O_2 172.36(6)
		O_2–Sb–O_2 93.04(6)
		O_2–Sb–O_2 74.06(6)

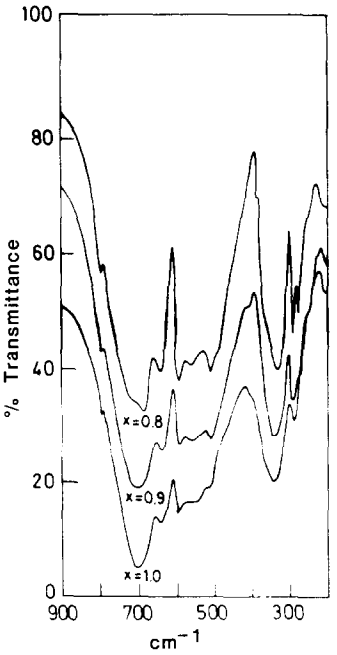

FIG. 3. IR absorption spectra of $Ti_{3(1-x)}Ni_xSb_{2x}O_6$ materials.

trirutile structures simultaneously, the rutile type (up to 66% in $x = 0.6$) being the majoritary component. On the other hand, IR spectra show a very intense broadening and the characteristic rutile type spectra appear in both cases ($x = 0.6$–0.7). Nevertheless, on the basis of the analogy in the space groups ($P4/mnm$) for rutile and trirutile structure types and the local symmetry (D_{4h}^{14}) in both cases, we can attribute the observed X-ray reflections and IR bands to a trirutile structure model. The procedure made recently (*17*) in the discussion of a transition α-PbO_2 (orthorhombic) rutile seems to be valid for our purposes. The possibility of an intergrowing of both structures in a single solid phase must be considered in this respect.

The temperature dependence of the molar magnetic susceptibility for $NiSb_2O_6$ is shown in Fig. 4. It can be observed that the susceptibility obeys a Curie–Weiss law behavior between 300 and 70 K and the ef-

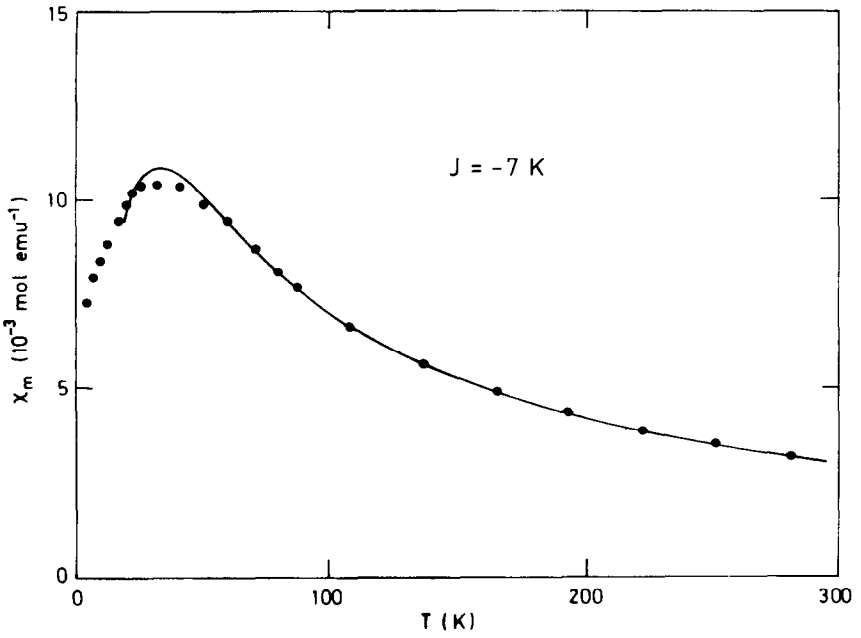

FIG. 4. The temperature dependence of the molar magnetic susceptibility for $NiSb_2O_6$.

fective magnetic moment obtained by a least-squares fit of the linear part of the (χ vs T) plot, which is 3.00 BM, agrees with $S = 1$. The susceptibility also shows a very broad maximum centered at 30 K, which indicates that an antiferromagnetic short range order of low dimensional nature is taking place.

This behavior can be attributed to the superexchange Ni–O–Ni at 160° intralayer interactions. However, this interaction involves at least one very long Ni–O distance and the bond angles Ni–O–Ni are quite different from 180° or 90°, for which the overlapping between the nickel and oxygen orbitals will decrease. Because of all this, the other possible interaction involving the next neighbors at 180°, Ni–O–O–Ni, along the square face diagonal of the basal plane in the trirutile structure could be very important (see Fig. 1b).

This seems to confirm the assumption stated earlier about the 2D magnetic ordering which appears to be a common feature of these oxides based in the trirutile-type structure.

Interlayer interactions producing a 3D order could be also present below the $T_{x\max.}$, as it has been reported earlier for the analogous $CoTa_2O_6$ oxide. At higher temperature the magnetic susceptibility data of $NiSb_2O_6$ have been analyzed using the high temperature series expansion method (HTSE) proposed by Rushbrooke and Wood (*18, 19*), for a square lattice layer system with free surfaces, that is, without magnetic neighbors above or below the layer. In a system with spin 1 antiferromagnetism the susceptibility is given to six orders in J/kT, by

$$\chi^{-1} = [3/S(S+1)] \cdot [kT/\mathrm{Ng}^2B^2][1 + 5.33(J/kT) + 9.77(J/kT)^2 + 13.27(J/kT)^3 + 19.06(J/kT)^4 + 45.09(J/kT)^5 + 25.46(J/kT)^6].$$

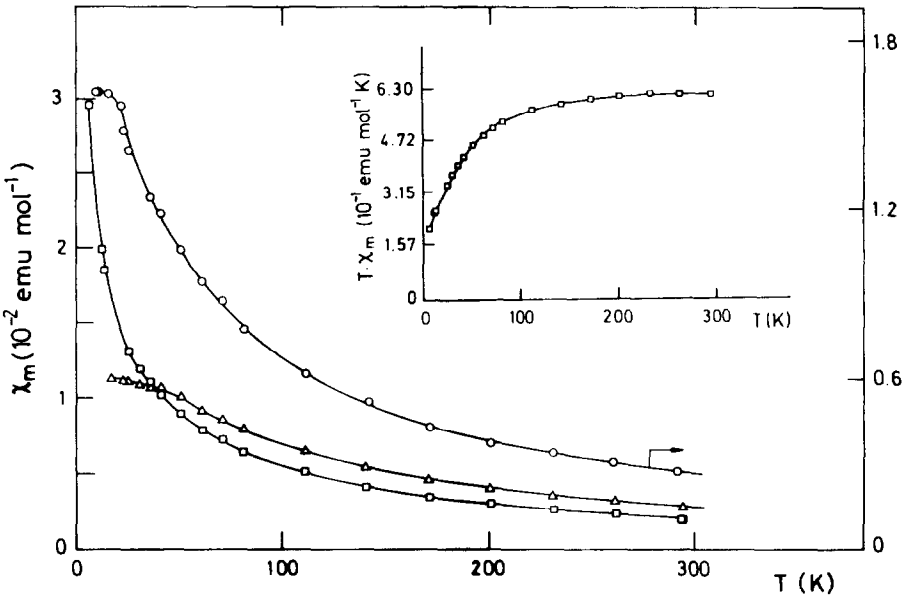

FIG. 5. The temperature dependence of the molar magnetic susceptibility for the isostructural doped $Ti_{3(1-x)}Ni_xSb_{2x}O_6$ oxides: $x = 0.9$ (△), $x = 0.8$ (○), and $x = 0.6$ (□). The inset shows $(\chi_m \cdot T)$ vs T.

The intrachain integral exchange constant, J, has been estimated by fitting the experimental data to the above equation. The fairly good agreement between experimental (solid circles) and calculated data (solid line) between 300 and 60 K yields a J/k value of -7 K (see Fig. 4).

The exchange integral J, which is proportional to the square of the transfer integral, is rather small because the Ni–O–Ni angle is 160° and under these conditions the overlap integral between nickel and oxygen is smaller than in the case of the K_2NiF_4 type structure for which this angle is 180° (*9*).

The magnetic susceptibility of the doped $Ti_{3(1-x)}Ni_xSb_{2x}O_6$ samples (Fig. 5) shows a very different behavior. At temperatures higher than 30 K the magnetic susceptibility follows a Curie–Weiss behavior for all the doped samples. The magnetic moments obtained are in good agreement with those expected for the nickel contribution and the Weiss constants are more negative when the value of $1.0 \geq x \geq 0.6$ increases. This shows that the antiferromagnetic interactions become less important when the nickel content diminishes.

For the composition $x = 0.9$ in the series $Ti_{3(1-x)}Ni_xSb_{2x}O_6$ the susceptibility exhibits a maximum at 30 K, and below this temperature the χ remains almost constant. The same fact is observed for $x = 0.8$ although the maximum in χ is obtained at 20 K, as can be observed in Fig. 5.

In the case of the $x = 0.6$ compound for which 40% of the Ni^{2+} has been replaced by the diamagnetic Ti^{4+} ion neither a maximum nor an inflexion point is observed in the (χ vs T) plot. The magnetic susceptibility obeys a Curie–Weiss behavior in the 300 to 20 K range and the calculated magnetic moment is 2.90 BM, which agrees with that expected for isolated Ni ions. Below 20 K small deviations of the linearity are observed, which is indicative that some antiferromagnetic interactions are still present; however, this effect is more significant when $\chi \cdot T$ vs T is plotted (Fig. 5, inset).

The decreasing of the $\chi \cdot T$ values at lower temperatures is observed with a value of only 0.38 emu · mol at 4.2 K, which confirms that at these low temperatures antiferromagnetic interactions are present.

Conclusions

Magnetic susceptibility measurements for the pure $NiSb_2O_6$ and for the isostructural $Ti_{3(1-x)}Ni_xSb_{2x}O_6$ oxides reveal in all cases the existence of short-range antiferromagnetic ordering probably followed, as it has been reported earlier in the case of the $CoSb_2O_6$, by a transition from short-to long-range order at lower temperatures for which the maximum in χ appears. The exchange integral J, calculated from the HTSE method, is -7 K, close to the value reported for $CoSb_2O_6$ (*20*).

The interactions have been analyzed by considering the next nearest neighbor 180° Ni–O–O–Ni superexchange interaction along one diagonal of the basal plane in the trirutile structure. Other possible interactions between nearest neighbors have been also considered although they involve at least one very long Ni–O distance and an Ni–O–Ni angle far from 180 or 90°, for which the overlapping of the orbitals is effective.

The Ni^{2+} and Sb^{5+} cations appear to be ordered as described because the antiferromagnetic interactions are still present even for the higher values of x corresponding to the composition $Ti_{1.2}Ni_{0.6}Sb_{1.2}O_6$.

More work is now in progress, mainly neutron diffraction experiments, in order to determine the magnetic structure and Néel temperatures of these compounds.

Acknowledgments

The authors acknowledge the financial support of DGICYT, M.E.C., Spain.

References

1. K. Brandt, *Arkiv. Kemi. Mineral. Geol.* **17a,** 1 (1943).
2. A. Grandin, M. M. Borel, C. Michel, and B. Raveau, *Mater. Res. Bull.* **18,** 239 (1983).
3. A. Grandin, M. M. Borel, C. Michel, N. Neguyen, and B. Raveau, *Mater. Chem. Phys.* **10,** 443 (1984).
4. M. Takano and T. Takada, *Mater. Res. Bull.* **5,** 449 (1970).
5. J. N. Reimers, J. E. Greedan, C. V. Stager, and Kremer, *J. Solid State Chem.* **83,** 20 (1989).
6. J. A. Alonso, A. Castro, A. Jerez, C. Pico, and M. L. Veiga, *J. Chem. Soc. Dalton Trans.*, 2225 (1985).
7. E. Ramos, M. Gaitan, A. Jerez, C. Pico, and M. L. Veiga. Reunión Quimica Inorganica, Toledo, Spain (1989).
8. J. Rodriguez-Carvajal, Program. Fullprof, III, Grenoble, France (1990).
9. F. Fernandez, Doctoral Thesis, Universidad Complutense, Madrid, Spain (1990).
10. M. L. Mulay (Ed.) "Magnetic Susceptibility," Wiley, New York (1963).
11. H. Kasper, *Mh. Chem.* **98,** 2107 (1967).
12. R. D. Shannon, *Acta Crystallogr.* **A32,** 751 (1976).
13. E. Husson, Y. Repelin, N. Quy Dao et H. Brusset, *Spectrochim. Acta,* **33A,** 995 (1977).
14. K. Hayashi, N. Noguchi, and M. Ishii, *Mater. Res. Bull.* **21,** 401 (1986).
15. C. Rocchiccioli-Deltcheff et Franck (Eds.) "L'Infrarouge en Chimie des Solides," Masson et Cie. Editeurs, Paris (1974).
16. C. Rocchiccioli-Deltcheff, T. Dupus, et C. Wadler, *C.R. Acad. Sci. Paris,* t.273 (1971).
17. G. Pourroy, E. Lutanie, and P. Plox, *J. Solid State Chem.* **86,** 41 (1990).
18. G. H. Rushbrooke and P. J. Wood, *Mol. Phys.* **1,** 257 (1958).
19. G. H. Rushbrooke and P. J. Wood, *Mol. Phys.* **6,** 409 (1963).
20. R. K. Kremer and J. E. Greedan, *J. Solid State Chem.* **73,** 579 (1988).